



## RESEARCH ARTICLE

### Photocatalytic activity of metal oxide/kaolinite nanocomposites under UV light irradiation

Perumal Mariselvi<sup>1</sup>, Paramasivan Parvathiraj<sup>2</sup>, & Thangaiya Anantha kumar<sup>3\*</sup>

<sup>1</sup> Department of Chemistry, Rani Anna Govt. College for Women, Tirunelveli, Tamil Nadu, India.

<sup>2</sup> Department of Zoology, Sri Ram Nallamani Yadava College of Arts and Science, Tenkasi, Tamil Nadu, India.

<sup>3</sup> Department of Chemistry, Merit Arts and Science College Idaikal, Tamil Nadu, India.

#### ARTICLE HISTROY

Received 16 November 2023

Revised 17 November 2023

Accepted 20 November 2023

#### Keywords

*Kaolinite*

*Titanium dioxide,*

*Methylene blue*

*Solvothermal*

*Photocatalysis*

#### ABSTRACT

Wastewater treatment, especially for industrial pollutants, may harm the environment. Many nations face a technological issue with textile, paper pulp, and other industries' colored wastewater disposal. Textile wastewater pollution is a major source of environmental pollution that taints and colors aquatic systems. The current study involved the investigation of the photocatalytic properties of TiO<sub>2</sub>/kaolinite nanocomposites by utilizing the solvothermal technique. The synthesized nanocomposites underwent additional characterization by the utilization of various analytical techniques, including X-ray diffraction, scanning electron microscopy with energy dispersive X-ray spectroscopy, atomic force microscopy, transmission electron microscopy and ultraviolet-visible absorption spectroscopy. The X-ray diffraction analysis indicates that during the creation of nanocomposites, the presence of the anatase phase of TiO<sub>2</sub> was detected in the TiO<sub>2</sub>/kaolinite composite. The scanning electron microscopy investigation revealed the presence of spherical morphology in the TiO<sub>2</sub>/kaolinite nanocomposites. The UV-Vis absorption margins exhibit a blue shift towards lower wavelengths, potentially attributed to the nanosize effect. The study assessed the photocatalytic performance of TiO<sub>2</sub>/Kaolinite nanocomposites by measuring the degradation of methylene blue dyes under UV light exposure. The results indicated that the application of swift heavy ion irradiation led to a notable improvement in the photocatalytic efficacy of the synthesized TiO<sub>2</sub>/Kaolinite nanocomposites in terms of degrading MB dyes.

✉ Anantha kumar  
[ananthspkc@gmail.com](mailto:ananthspkc@gmail.com)

©2023 The Author(s). Published by Panainool Ltd.

## Introduction

According to the definition given in the context of chemistry, nanoscale materials are structures with a size between 1 and 100 nm. In recent years, these materials have helped to accelerate the



development of nanoscience and nanotechnology (Joudeh & Linke, 2022). As of right now, titanium dioxide ( $\text{TiO}_2$ ) nanoparticles are minuscule fragments of the inorganic molecule. Usually ranging in size from 1 to 100 nanometers, they possess distinct characteristics when contrasted with titanium dioxide in bulk (Khan et al., 2022).  $\text{TiO}_2$  nanoparticles are highly reactive and valuable in a range of applications because of their small size and enormous surface area relative to their volume (Musial et al., 2020).  $\text{TiO}_2$  nanoparticles usually appear in paints, coatings, ceramics, and sunscreens and cosmetics (Irshad et al., 2021). Additionally, they have potential uses in the biomedical, catalysis, water treatment, and self-cleaning surfaces (Waghmode et al., 2019).

Materials that consist of a mixture of clay particles and titanium dioxide ( $\text{TiO}_2$ ) nanoparticles are known as clay nanocomposites. Typically, layered silicate minerals like illite, montmorillonite, and kaolinite form the clay particles (Serwicka, 2021). The application of clays including montmorillonite, rectorite, and kaolinite in the treatment of waste water has garnered significant interest in recent years (Chuaicham et al., 2023). Naturally occurring materials have the ability to absorb organic compounds either on their external surfaces or within their interlaminar regions through processes of contact or replacement (Isa et al., 2022). In addition, these structures possess layered arrangements, extensive surface areas, and notable capacities for cation exchange. According to reports,  $\text{TiO}_2$  particle dispersion into layered clays can enhance catalytic performance because the architectures of these composites can stabilise  $\text{TiO}_2$  crystals, making

them accessible to a variety of molecules (Chuaicham et al., 2023; Hamidi & Aslani, 2019).  $\text{TiO}_2$  nanoparticles can be intercalated into the layers of the clay mineral or dispersed in a clay solution to create these nanocomposites. The ability of  $\text{TiO}_2$ /clay nanocomposites to enhance the individual component's qualities is one of its key advantages (Chuaicham et al., 2023). While the  $\text{TiO}_2$  nanoparticles can improve the optical, catalytic activity, electrical property, and photocatalytic characteristics of the clay, the clay particles can improve the  $\text{TiO}_2$ 's mechanical strength and thermal stability (Dharma et al., 2022). Researchers have already looked into the antibacterial, structural, and morphological properties of Kaolinite/ $\text{TiO}_2$  nanocomposites (R. Li et al., 2020; Xie et al., 2022). It is the goal of this study to use the solvothermal method to make metal oxide/clay nanocomposites, which will then be used to get rid of the methylene blue dye.

## Materials and method

### *Preparation of $\text{TiO}_2$ /Kaolinite Nanocomposites*

1% w/w clay-water dispersion was agitated for two hours. 70% w/w  $\text{TiO}_2$  content was reached by adding a small amount of  $\text{TiO}_2$  solvent to the mixture. This was done over the course of a day. After that, the mixture was spun at 3,800 rpm for ten minutes. Three times of centrifugation were done after ultrapure water was used to clean the dry phase. The finished clay- $\text{TiO}_2$  mix was mixed in a solution of 1:1 water to ethanol. It was then heated at 180 °C for five hours in an autoclave to treat it hydrothermally. The item was spun at 3,800 rpm for another 15 minutes and then dried

in a 60 °C oven for 3 hours (Undabeytia et al., 2021).

### **Instrumental Characterizations**

For X-ray diffraction (XRD) measurements, a Philips diffractometer made by the "X" company was used with radiation that was monochromatized Cu K $\alpha$  ( $\lambda=1.54060 \text{ \AA}$ ). Scherrer's analysis of X-ray diffraction (XRD) is a widely employed method for the assessment of crystallite size. All absorbance measurements in the range of 200 nm to 800 nm were conducted using a Jascow-500 double-beam UV-Vis spectrophotometer equipped with quartz cells with an optical path length of 1 mm. The scanning electron microscopy (SEM) image was acquired using the HITACHI-S-3400H model. The transmission electron microscopy (TEM) investigation was conducted using a Philips CM-200 electron microscope, which operated at a voltage of 200 KV and had a resolution of 2.4  $\text{\AA}$ . Atomic force microscopy (AFM) provides exceptional precision in the determination of particle sizes, operating by physically scanning materials at a sub-micron scale with a probe tip of atomic dimensions.

### **Photocatalytic activity of Nanocomposites**

Methylene blue dye solutions are prepared and introduced into a UV multilamp photoreactor tube. The dye solution was supplemented with the necessary quantity (20 mg) of produced material. To achieve adsorption-desorption equilibrium, the dye solutions were dark-conditioned for thirty minutes prior to irradiation. It was then stored for

30 minutes within the UV multilamp photoreactor. Prior to the UV-visible absorption tests, the collected liquid underwent centrifugation and filtration. The following formula was used to predict the dye's rate of degradation,

$$\text{Removal percentage (\% R)} = \frac{[C_i - C_f / C_i] \times 100}{\text{-----}} \text{---(1)}$$

Where,  $C_i$  and  $C_f$  is the initial and final dye concentration in ppm at a given time.

## **Results and Discussion**

### **XRD analysis of TiO<sub>2</sub>/Kaolinite Nanocomposites**

Fig. 1 displays the XRD pattern of the TiO<sub>2</sub>/Kaolinite nanocomposites made using a solvothermal technique. The (101), (004), (200), (105) and (204) planes are given to the sharper and stronger diffraction peaks in Figure 1. These peaks are found at 25.5°, 37.8°, 47.9°, 53.59°, and 62.36°. The X-ray diffraction pattern exhibited a high degree of concordance with the JCPDS file 21-1272, indicating that all the peaks observed can be attributed to the presence of anatase phases of titanium dioxide (Baltabayeva et al., 2021; Damkale et al., 2021). The high purity of the nanocomposite samples is indicated by the absence of any further impurity peaks. The resulting products exhibit high crystallinity, as seen by the strong and crisp diffraction peaks. This finding confirms that clay/metal oxide development is occurring. The dimensions of nanocomposites were determined using the Debye-Scherrer formula. The size of the crystals was determined to be 81.61 nm.

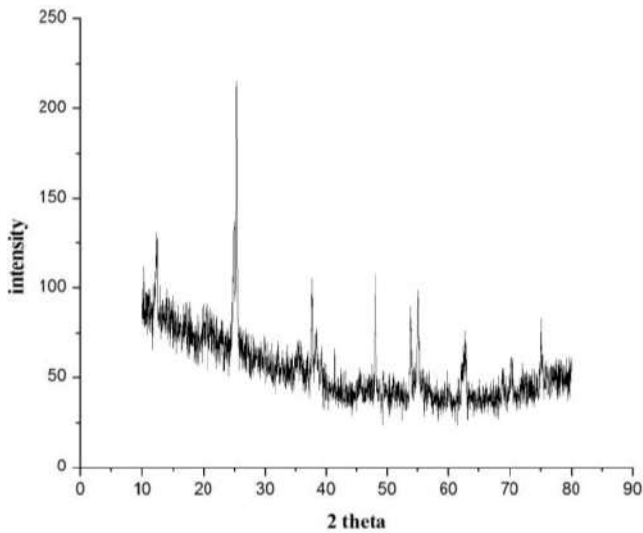


**Fig.1.** XRD pattern of  $\text{TiO}_2/\text{Kaolinite}$  nanocomposites

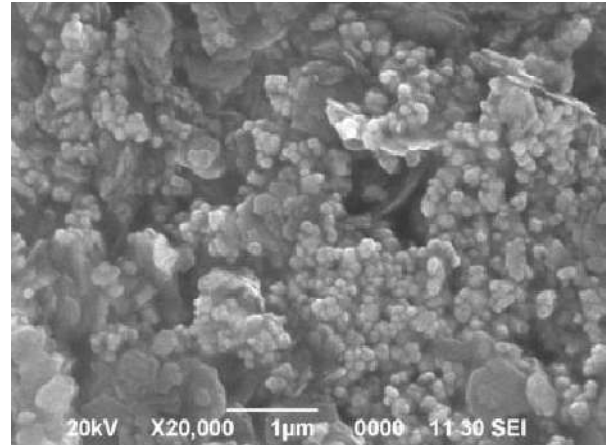


**Fig.2.** SEM image of  $\text{TiO}_2/\text{Kaolinite}$  nanocomposites

### **SEM with EDAX analysis of $\text{TiO}_2/\text{Kaolinite}$ Nanocomposites**

The morphological surface of  $\text{TiO}_2/\text{Kaolinite}$  nanocomposites was examined using SEM. The nanocomposites in Fig. 2 SEM picture have an agglomeration nanocomposites shape and are generally spherical and spongy. The sample under investigation's SEM picture demonstrated a matrix made up of sub-micron  $\text{TiO}_2$  particles adhered to the clay matrix's surface and micro-sized kaolinite particles with a layered structure. The SEM images of the proven matrix, which included sub-micron  $\text{TiO}_2$  particles adhered to the clay matrix's surface and micro-sized kaolinite particles with a layered structure, were reported by (Samuvel Raj et al., 2023). Musial et al., (2020) also reported the similar observation. An EDAX spectrum of the material is shown in Fig.2a. These studies using EDAX show that the sample has the right amounts of Ti, O, Al, and Si in prepared sample was recorded in elemental composition analysis.

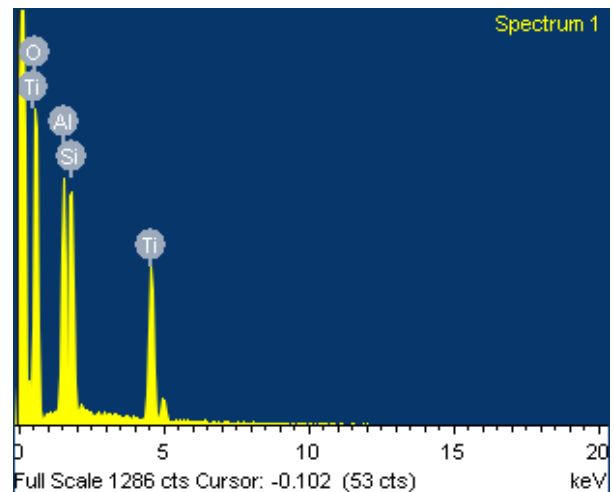


**Fig.2.a.** EDAX image of  $\text{TiO}_2/\text{Kaolinite}$  nanocomposites

### **AFM analysis of $\text{TiO}_2/\text{Kaolinite}$ Nanocomposites**

An essential tool for any study on nanoscale phenomena is AFM. The figure shows the AFM picture of metal oxide/clay nanocomposites that were created using a solvothermal process (Fig.3). For this sample, the micrograph at  $5\ \mu\text{m} \times 5\ \mu\text{m}$  shows a consistent distribution of cone-shaped grains covering the nanocomposites surface. The particle's homogeneous dispersion and nanometer-sized size have been noted. Using AFM

investigation, the surface roughness, heights, and RMS average value were ascertained. The XRD result and the metal oxide/clay nanocomposites are in good agreement. The very uniform distribution of spherically shaped particles was observed by (Asamoah et al., 2020; Joudeh & Linke, 2022). The statistical roughness analysis (CSPM) showed that the surface skewness was -0.0806, the surface kurtosis was 2.47, the average roughness was 0.422 nm, and the root mean square roughness was 0.513 nm.

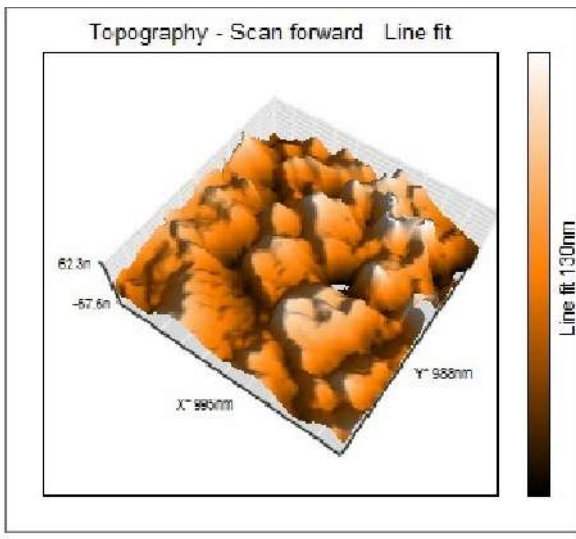


**Fig.3.** AFM image of TiO<sub>2</sub>/Kaolinite nanocomposites

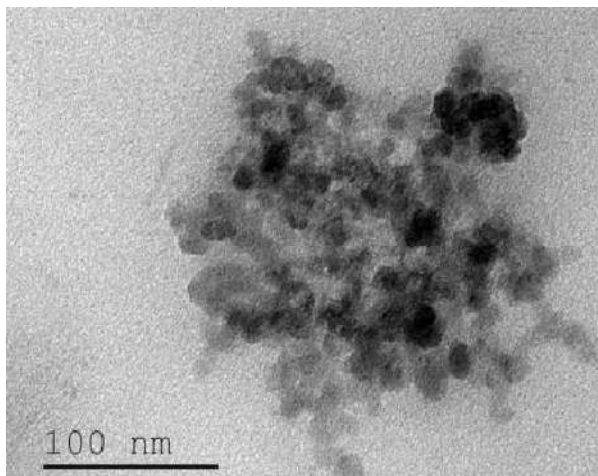


**Fig.4.** TEM image of TiO<sub>2</sub>/Kaolinite nanocomposites

**TEM analysis of TiO<sub>2</sub>/Kaolinite Nanocomposites**

Confirmation of the particle size, growth pattern, and crystallite distribution was achieved using transmission electron spectroscopy investigation. A representative TEM picture of the TiO<sub>2</sub>/Kaolinite nanocomposites is shown in Fig. 4. The particles' comparatively homogeneous particle size distribution is evident. Based on the TEM picture, the nanocomposites' average size is approximately 50 nm.

**UV-Vis Absorption Spectroscopy**

Figure 5 displays the UV-Vis absorption spectrum of TiO<sub>2</sub>/Kaolinite nanocomposites. The absorption characterisation of nanoparticles is a valuable tool. The wavelength range for the UV-Vis spectral study was 200–800 nm. Using the following formula (Agustina et al., 2021), we can find the optical band gap (E<sub>g</sub>) with the use of absorption spectroscopy.

$$\alpha = (h\nu - E_g) / 2h\nu \dots \dots \dots (2)$$

In this context, the symbol *hν* represents the energy of a photon, while  $\alpha$  and *n* are constants. In the case of a direct energy gap, the value of *n* is 2, while for an indirect energy gap, the value of *n* is 1/2.

TiO<sub>2</sub>/Kaolinite nanocomposites exhibit a blue shift in the absorption edge and a corresponding band gap of 3.3 eV, as illustrated in Figure 5.a. The produced TiO<sub>2</sub>/Kaolinite nanocomposites have band gap energy of 3.3 eV, which is higher than the 3.2 eV value of the bulk TiO<sub>2</sub>. This makes sense because it has been discovered that the semiconductor's band gap depends on particle size

(Almatroudi, 2020). Comparing these nanocomposites to bulk TiO<sub>2</sub>, they exhibit blue shift, or increased energy. The structural flaws in nanomaterials and the influence of nanosize may be the source of the blue shift (D. Li et al., 2020).

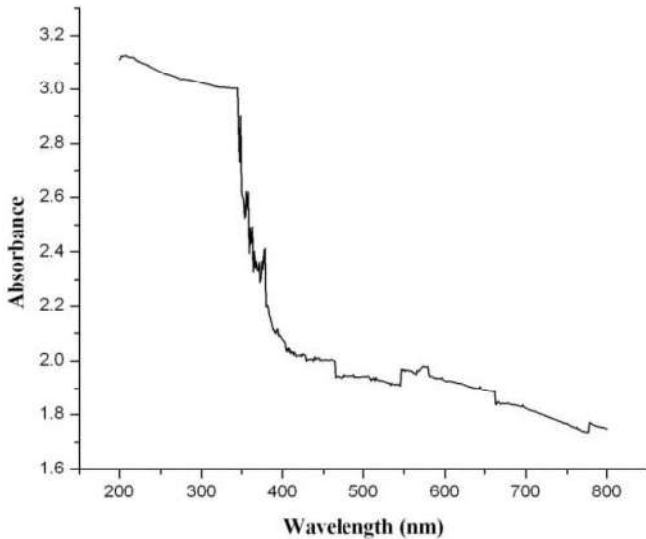


**Fig.5.** UV-Vis absorption spectrum of TiO<sub>2</sub>/Kaolinite nanocomposites

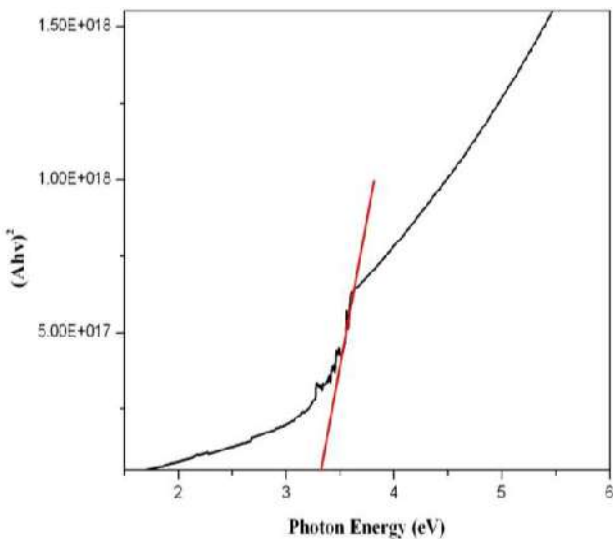


**Fig.5.a.** Band gap energy of TiO<sub>2</sub>/Kaolinite nanocomposites

**Photocatalytic activity of TiO<sub>2</sub>/Kaolinite Nanocomposites**

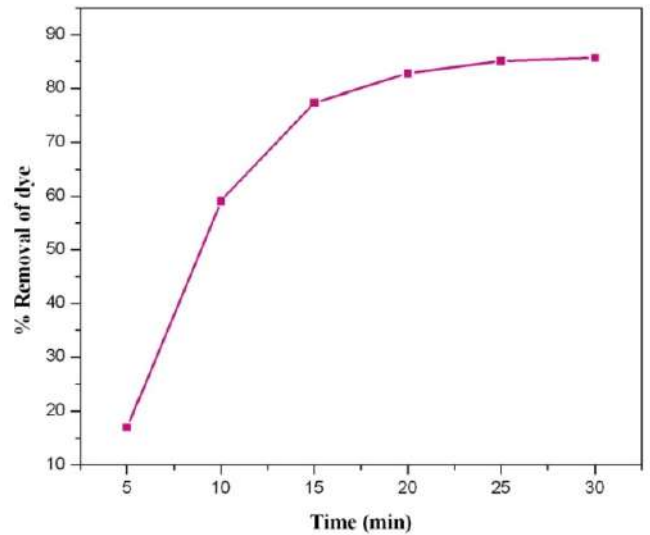
*Effect of contact time*

Figure 6 illustrates the way time variation affects MB dyes. The percentage of dye removed also rises with time. Based on the experimental findings, it can be observed that the photocatalytic degradation of MB dye exhibits a tendency to adhere to pseudo-first-order kinetics, with the following equation providing the rate expression:

$$\ln (C_0/C_t) = kt \dots\dots\dots (3)$$

Where, C<sub>0</sub> = initial concentration of the dye

C<sub>t</sub> = final concentration of the dye in various time interval.



**Fig.6.** Effect of Contact time

*Effect of pH*

The pH levels of waste water from the textile industry typically vary greatly. Moreover, pH influences the production of hydroxyl radicals .For MB dye, the pH ranges from 3 to 11. TiO<sub>2</sub> has a

zero point charge of 6.25. Increases in MB dye pH from 3 to 11 resulted in better percentage elimination (under fundamental conditions). The catalyst's surface will become negatively charged in this state. Therefore, the catalyst readily attracted the MB dye. The illustration appears in Fig.7.

*Effect of Dose Variation*

Catalyst concentrations ranged from 12 mg to 20 mg. Figure 8 shows that as the amount of photocatalyst climbed, the efficiency seemed to go up. This is likely because there were more active sites for the photocatalytic reaction on the surface. When the photocatalyst is overdosed, however, the number of active sites on its surface may stay about the same. This is because more light is scattered, less light can pass through, and the surface area is lost because of solids sticking together at high concentrations.

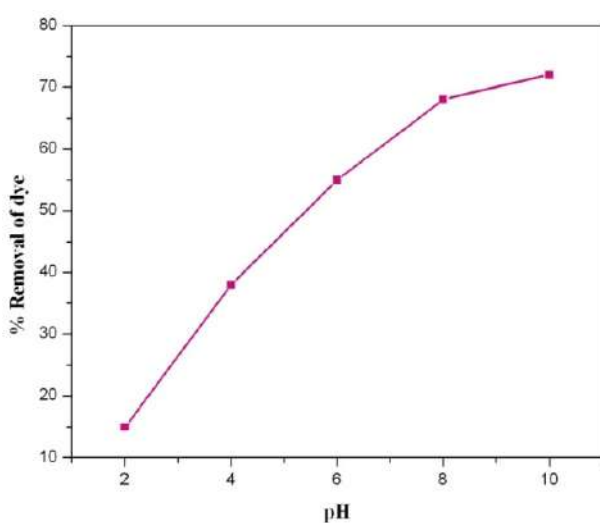


**Fig.7.** Effect of pH on MB dye

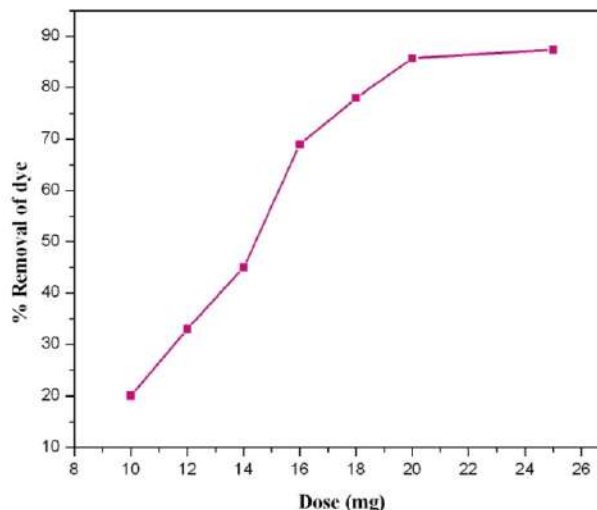


**Fig.8.** Effect of different dose concentrations of photocatalytic reaction

*Effect of concentration of dyes*

Under UV light systems, methylene blue was photocatalytically decolorated at varying starting concentrations ranging from 10 ppm to 50 ppm. The percentage of elimination reduced as dye molecule concentrations increased. Because of the surface of the photocatalyst absorbs a greater quantity of dye molecules. As a result, the photon entry channel will be shortened. The methylene blue dyes' breakdown, as depicted in fig. 9.

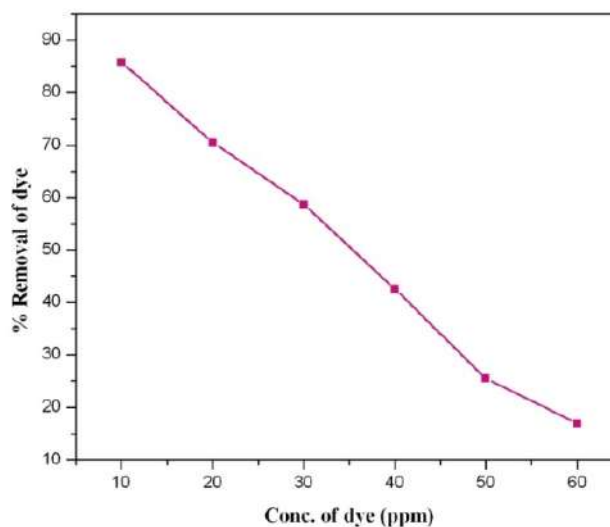


**Fig.9.** Effect of Initial Concentration of dye



## Conclusion

Overall, the synthesis of titanium dioxide/kaolinite nanocomposites has been effectively achieved by the solvothermal approach. The produced nanocomposites underwent characterization using a range of analytical techniques, including X-ray diffraction, scanning electron microscopy with energy-dispersive X-ray spectroscopy, atomic force microscopy, transmission electron microscopy, and ultraviolet-visible absorption spectroscopy. The X-ray diffraction analysis indicated the existence of the anatase crystalline phase of titanium dioxide (TiO<sub>2</sub>). The samples were subjected to characterization in terms of their size and morphology by the utilization of scanning and transmission electron microscopy techniques, respectively. The composite material exhibits band gap energy of 3.3 eV, surpassing the bulk TiO<sub>2</sub>'s value of 3.2 eV. The nanocomposites exhibit a blue shift, indicating a higher energy state in comparison to the bulk TiO<sub>2</sub>. The data obtained from the decolorization reactions of the metal oxide/clay nanocomposite demonstrated a good fit with the pseudo-first-order kinetic model. The investigation indicates that the materials obtained possess significant utility in the field of water treatment.

## Acknowledgement

The authors' thankful to the Department of Chemistry, Merit Arts and Science College Idaikal, Tamil Nadu, for providing necessary facilities for carried out of this work.

## References

- Agustina, T. E., Handayani, W., & Imawan, C. (2021). The UV-VIS Spectrum Analysis From Silver Nanoparticles Synthesized Using *Diospyros maritima* Blume. Leaves Extract . *Proceedings of the 3rd KOBI Congress, International and National Conferences (KOBICINC 2020)*, 14(Kobicinc 2020), 411–419. <https://doi.org/10.2991/absr.k.210621.070>
- Almatroudi, A. (2020). Silver nanoparticles: synthesis, characterisation and biomedical applications. *Open Life Sciences*, 15(1), 819–839. <https://doi.org/10.1515/biol-2020-0094>
- Asamoah, R. B., Yaya, A., Nbelayim, P., Annan, E., & Onwona-Agyeman, B. (2020). Development and Characterization of Clay-Nanocomposites for Water Purification. *Materials (Basel, Switzerland)*, 13(17). <https://doi.org/10.3390/ma13173793>
- Baltabayeva, B., Ospanova, A., & Kubasheva, Z. (2021). Preparation of nanocomposite silver/kaolin with antibacterial properties. *MATEC Web of Conferences*, 340, 01030. <https://doi.org/10.1051/mateconf/202134001030>
- Chuaicham, C., Trakulmututa, J., Shu, K., Shenoy, S., Srikaow, A., Zhang, L., Mohan, S., Sekar, K., & Sasaki, K. (2023). Recent Clay-Based Photocatalysts for Wastewater Treatment. *Separations*, 10(2). <https://doi.org/10.3390/separations10020077>
- Damkale, S. R., Arbuj, S. S., Umarji, G. G., Rane, S. B., & Kale, B. B. (2021). Highly crystalline anatase TiO<sub>2</sub>nanocuboids as an efficient photocatalyst for hydrogen generation. *RSC Advances*, 11(13), 7587–7599. <https://doi.org/10.1039/d0ra10750f>
- Dharma, H. N. C., Jaafar, J., Widiastuti, N., Matsuyama, H., Rajabsadeh, S., Othman, M. H. D., Rahman, M. A., Jafri, N. N. M., Suhaimin, N. S., Nasir, A. M., & Alias, N. H. (2022). A Review of Titanium Dioxide (TiO<sub>2</sub>)-Based Photocatalyst for Oilfield-Produced Water Treatment. *Membranes*, 12(3). <https://doi.org/10.3390/membranes12030345>
- Hamidi, F., & Aslani, F. (2019). TiO<sub>2</sub>-based Photocatalytic Cementitious Composites:





- Materials, Properties, Influential Parameters, and Assessment Techniques. *Nanomaterials*, 9(10). <https://doi.org/10.3390/nano9101444>
- Irshad, M. A., Nawaz, R., ur Rehman, M. Z., Adrees, M., Rizwan, M., Ali, S., Ahmad, S., & Tasleem, S. (2021). Synthesis, characterization and advanced sustainable applications of titanium dioxide nanoparticles: A review. *Ecotoxicology and Environmental Safety*, 212, 111978. <https://doi.org/https://doi.org/10.1016/j.ecoenv.2021.111978>
- Isa, A., Nosbi, N., Che Ismail, M., Md Akil, H., Wan Ali, W. F. F., & Omar, M. F. (2022). A Review on Recycling of Carbon Fibres: Methods to Reinforce and Expected Fibre Composite Degradations. *Materials (Basel, Switzerland)*, 15(14). <https://doi.org/10.3390/ma15144991>
- Joudeh, N., & Linke, D. (2022). Nanoparticle classification, physicochemical properties, characterization, and applications: a comprehensive review for biologists. *Journal of Nanobiotechnology*, 20(1), 262. <https://doi.org/10.1186/s12951-022-01477-8>
- Khan, Y., Sadia, H., Ali Shah, S. Z., Khan, M. N., Shah, A. A., Ullah, N., Ullah, M. F., Bibi, H., Bafakeeh, O. T., Khedher, N. Ben, Eldin, S. M., Fadhl, B. M., & Khan, M. I. (2022). Classification, Synthetic, and Characterization Approaches to Nanoparticles, and Their Applications in Various Fields of Nanotechnology: A Review. *Catalysts*, 12(11). <https://doi.org/10.3390/catal12111386>
- Li, D., Song, H., Meng, X., Shen, T., Sun, J., Han, W., & Wang, X. (2020). Effects of Particle Size on the Structure and Photocatalytic Performance by Alkali-Treated TiO<sub>2</sub>. *Nanomaterials*, 10(3). <https://doi.org/10.3390/nano10030546>
- Li, R., Li, T., & Zhou, Q. (2020). Impact of Titanium Dioxide (TiO<sub>2</sub>) Modification on Its Application to Pollution Treatment—A Review. *Catalysts*, 10(7). <https://doi.org/10.3390/catal10070804>
- Musial, J., Krakowiak, R., Mlynarczyk, D. T., Goslinski, T., & Stanisz, B. J. (2020). Titanium Dioxide Nanoparticles in Food and Personal Care Products—What Do We Know about Their Safety? *Nanomaterials*, 10(6). <https://doi.org/10.3390/nano10061110>
- Samuvel Raj, R., Prince Arulraj, G., Anand, N., Kanagaraj, B., Lubloy, E., & Naser, M. Z. (2023). Nanomaterials in geopolymer composites: A review. *Developments in the Built Environment*, 13, 100114. <https://doi.org/https://doi.org/10.1016/j.dibe.2022.100114>
- Serwicka, E. M. (2021). Titania-Clay Mineral Composites for Environmental Catalysis and Photocatalysis. *Catalysts*, 11(9). <https://doi.org/10.3390/catal11091087>
- Undabeytia, T., Shuali, U., Nir, S., & Rubin, B. (2021). Applications of Chemically Modified Clay Minerals and Clays to Water Purification and Slow Release Formulations of Herbicides. *Minerals*, 11(1). <https://doi.org/10.3390/min11010009>
- Waghmode, M. S., Gunjal, A. B., Mulla, J. A., Patil, N. N., & Nawani, N. N. (2019). Studies on the titanium dioxide nanoparticles: biosynthesis, applications and remediation. *SN Applied Sciences*, 1(4), 310. <https://doi.org/10.1007/s42452-019-0337-3>
- Xie, Y., Wang, J., Ren, F., Shuai, H., & Du, G. (2022). Nonmetallic Mineral as the Carrier of TiO<sub>2</sub> Photocatalyst: A Review. *Frontiers in Catalysis*, 2(March), 1–11. <https://doi.org/10.3389/fctls.2022.806316>